Food & Function

ROYAL SOCIETY OF CHEMISTRY

PAPER

View Article Online
View Journal | View Issue

Cite this: *Food Funct.*, 2024, **15**, 9524

Effect of heat-treated flaxseed lignan macromolecules on the interfacial properties and physicochemical stability of α-linolenic acid-enriched O/W emulsions†

Chen Cheng,[a,b] Xiao Yu,[b,c] Fenghong Huang,[b] Lei Wang,[b] Zhenzhou Zhu,*[a] Jing Yang,[b] Peng Chen[b] and Qianchun Deng *[b]

Flaxseed lignan macromolecules (FLMs) are important polyphenols present in flaxseeds with interfacial adsorption behavior. However, FLMs are easily degraded during thermal treatment in emulsions, which further influences their interfacial properties and application. In this work, the interfacial properties of FLMs between oil and water were evaluated using compression isotherms and interfacial tension to investigate the regulation mechanism of FLMs and their heat-treated products on the stability of O/W emulsions. Furthermore, the improvement mechanism of FLM heat-treated products on the physicochemical stability of flaxseed oil emulsions was clarified. Studies showed that thermal degradation occurred on terminal phenolic acids in FLMs when treated under 100 and 150 °C (FLM-100 and FLM-150) without any decrease in antioxidant activity. FLM-100 and FLM-150 improved the physicochemical stability of sunflower lecithin (S90)-stabilized flaxseed oil emulsions and reduced the concentration of hydroperoxides and TBARS by 26.7% and 80% ($p < 0.05$), respectively, during storage. This was due to the high interfacial anchoring of FLM-100 and FLM-150, which further strengthened the interface of oil droplets and improved the interfacial antioxidant effect of FLMs. This implies that FLM-100 and FLM-150 could act as new efficient antioxidants for application in food emulsions.

Received 5th June 2024,
Accepted 17th August 2024

DOI: 10.1039/d4fo02663b

rsc.li/food-function

1. Introduction

Flaxseed oil (FO) is one of the richest sources of α-linolenic acid (ALA)—an essential fatty acid. Epidemiological surveys indicated that ALA plays a crucial role in human health throughout the entire lifecycle, including brain development in babies, the fertility of men and women, and the prevention of neurodegenerative diseases in the elderly.[6] ALA can be metabolized into higher activity long-chain n-3 polyunsaturated fatty acids (n-3 PUFAs), such as docosahexaenoic acid (DHA), eicosapentaenoic acid (EPA) and other n-3 derivatives in mammals.[6] However, due to ALA's low water solubility, high oxidation susceptibility, and limited *in vivo* conversion into DHA and EPA, the effective intervention dose of ALA was calculated to exceed the normal intake. More importantly, reports proved that enterolactone, the metabolite of secoisolariciresinol (SECO), could regulate ALA metabolism by promoting the extracellular efflux of free fatty acids (FFAs) and triglycerides (TAGs) and decreasing the expression of fatty acid β-oxidation-related protein (CPT1).[9] Therefore, it also could be a wonderful antioxidant for the design of FO-enriched food.[7,8]

Lignans refer to a series of plant secondary metabolites that are formed *via* the polymerization of two phenylpropanoid (C6–C3) derivatives in various configurations, existing as dimers, trimers, and polymers in plants. Approximately 769 lignans have been isolated and identified over the past few years; among them, flaxseed lignan has been found to have the highest content in nature.[1] Flaxseed lignan exists in flaxseed hull as an SDG copolymer structure, which is named the flaxseed lignan macromolecule (FLM). The FLM is surrounded by flaxseed kernel and can protect FO from oxidation and other external environment attack. Considering the natural

[a]*National R&D Center for Se-rich Agricultural Products Processing, Hubei Engineering Research Center for Deep Processing of Green Se-rich Agricultural Products, School of Modern Industry for Selenium Science and Engineering, Wuhan Polytechnic University, Wuhan 430023, China. E-mail: zhenzhou.zhu@whpu.edu.cn; Tel: +86-27-86827874*
[b]*Oil Crops Research Institute of the Chinese Academy of Agricultural Sciences, Hubei Key Laboratory of Lipid Chemistry and Nutrition and Key Laboratory of Oilseeds Processing, Oil Crops and Lipids Process Technology National & Local Joint Engineering Laboratory, Wuhan 430062, China. E-mail: dengqianchun@caas.cn*
[c]*College of Food and Bioengineering, Henan Key Laboratory of Cold Chain Food Quality and Safety Control, Zhengzhou University of Light Industry, Zhengzhou 450001, China*

† Electronic supplementary information (ESI) available. See DOI: https://doi.org/10.1039/d4fo02663b

structure of the FLM, it occurs as a linear copolymer ester-linked by 3-hydroxy-3-methylglutaric acid (HMGA), and its skeleton comprises SDG and a few flavonoid glycosides (*e.g.*, pinoresinol diglucosides (PDGs) and herbacetin diglucoside (HDG)), among which HDG/PDG predominantly existed with a FerAG moiety in longer chain FLMs, which may further influence the biosynthesis of these longer chain variants of FLMs. Besides, ferulic acid glucoside (FeAG), *p*-coumaric acid glucoside (CouAG) or caffeic acid glucoside (CafAG) was grafted at terminals for the formation of complete FLMs.[5] The critical role of flaxseed lignans in preventing multiple chronic diseases has been well confirmed, including reducing the risk of cardiovascular diseases, type 2 diabetes, and different types of cancers.[2] Pharmacokinetic parameters for SDG and FLM have been previously evaluated in female Wistar rats after a single oral dose.[14] The study indicated that the total enterolactone and enterodiol (final metabolite of FLM and SDG) reached similar maximum concentrations between 11 and 12 h, and the total body exposures were similar for both enriched SDG and FLM. Considering the economy and safety of the application of flaxseed lignans, FLMs can serve as cost-effective alternatives to the SDG due to their pharmacokinetic characteristics.[5]

To achieve the co-delivery of ALA and flaxseed lignans, an emulsion system can be designed due to its high tolerance for both lipophilic and hydrophilic bioactive substances.[2,7] Compared with other emulsifiers, phospholipids could motivate the activity of lipolytic enzymes and participate in the micellization process of bile salts, free fatty acids, monoglycerides, *etc.*, which promoted the absorption of ALA.[10] When co-absorbed with ALA, phospholipids were reported to improve transportation and metabolism by promoting the expression of the protein that is related to the formation and exocytosis of chylomicrons.[8] Therefore, co-intake of flaxseed lignans and ALA by phospholipid-stabilized FO emulsions could improve the bioaccessibility of ALA *via* decreasing consumption by inhibiting ALA oxidation, enhance the absorption of ALA by promoting the formation of ALA micelles, and improve the metabolism of ALA (to EPA/DHA) through decreasing β-oxidation.

FLM has also been recently promoted as a nutraceutical with known safety effects and has generally been employed in commercial products such as plant milk, bread, coarse grain biscuits, and mooncakes.[2,3] However, the release of lignans was seriously limited during digestion due to the remaining integral cell structure for flaxseeds or sesame powder. It has been proved that the daily intake of more than 500 mg per day lignans is likely to play their biological activity.[4] However, the daily intake of lignans from flaxseed products ranged from 300 to 500 mg per day for secoisolariciresinol diglucoside (SDG) for most populations, resulting in the insufficient intake dose to develop a significant dose-effect relationship for adults.[4,5] Therefore, with the wide concern for a healthy life, the delivery efficiency of FLM in FO emulsion is also an important research field. Besides, thermal processing is a common and necessary process in the manufacture of lignan-enriched foods such as pasteurization, boiling, cooking and roasting. From modest heat treatments, the input of thermal energy can exert significant effects on the content, structure of food polyphenols due to their degradation, solubilization and mutual effects with other food components.[11] For example, for sesamin and sesamol-enriched sesame meal, thermal processing (240 °C for 20 min) increased the release of lignans (sesamin and sesamol) to 19.6% after *in vitro* digestion due to the degradation of aglycones and glycosides.[12] The batch pasteurization (85 °C for 20 min) for SDG-enriched whey drinks does not affect the content of SDG.[13] However, the concentration of SDG degraded by 25% after 6 months of storage under 8 °C.[13] However, there is no in-depth study on the structural and functional changes of FLMs under different heat treatments, particularly for the structure–function (antioxidant activity) relationship and the microscopic behavior changes in emulsions. Therefore, it was urgent to investigate the structural and functional changes of FLMs under different thermal processes and strive to achieve the optimal use of lignans in the food industry.

Accordingly, low-temperature drying (37 and 55 °C), pasteurization (70 °C), boiling (100 °C) and baking (150 °C) temperatures are set to simulate different process temperatures of FLMs. The antioxidant activity of heat-treated/untreated FLMs is detected and further analyzed based on their structural and composition changes. Furthermore, a previous study has proved that using phospholipids as emulsifiers to prepare an emulsion delivery system could improve the release and absorption of ALA compared with proteins and polysaccharides.[8] Therefore, sunflower lecithin-stabilized FO emulsion was selected to evaluate the effect of heat-treated/untreated FLM on the physicochemical stability, focusing on the interfacial antioxidant theory. This study aims to develop effective plant-based antioxidants, which can be further applied in functional foods and beverages.

2. Materials and methods

2.1 Chemicals and reagents

FO was obtained from Hongjingyuan Oil Co. Ltd (Xilingol, China). Sunflower lecithin Sunlipon™ 90 (S90) was provided by a commercial supplier (Perimondo, New York, NY, USA) Secoisolariciresinol diglycoside (SDG, 97%), secoisolariciresinol (SECO, 95%), thiobarbituric acid (TBA), 1,1,3,3-tetraethoxypropane, sodium azide, cumene hydroperoxide, 2,2-azobis-2-methylpropanimidamide dihydrochloride (AAPH), lipase (from porcine pancreas), and bile extract (porcine) were offered by Sigma-Aldrich (Saint Louis, MS, USA). Other reagents were purchased from Sinopharm Chemical Reagent Co., Ltd (Beijing, China).

2.2 Extraction of FLM

In brief, flaxseed hull powder (FHP, 20 g) was defatted by incubating with 100 mL *n*-hexane at 25 °C for 24 hours. Then, defatted FHP (20 g) was subjected to three extractions using 100 mL of 70% ethanol (v/v) for 24 hours. After each extrac-

tion, the mixture was centrifuged at 10 000*g* for 40 minutes. The FLM-enriched supernatant obtained from each extraction was obtained using a C18 solid-phase extraction column (Waters, C18, 5 cm) to purify polar small-molecule polyphenols. The purified FLM was concentrated using a rotary evaporator (IKARV10D, Germany), followed by drying using a vacuum freeze dryer, and then stored at −18 °C for in-depth analyses.

2.3 Preparation of heat-treated FLMs

FLMs were re-dissolved in 0.5 mL 70% ethanol water (v/v) and then diluted to 10 mL with distilled water (5 mg mL^{-1}, w/v). Subsequently, FLM solutions were heated in a water bath at 37, 55, 70, and 100 °C for 30 min to simulate different heating processes, low-temperature drying (55 °C), pasteurization (70 °C), and boiling (100 °C), respectively. Moreover, the temperature of 150 °C in the oil bath for 30 min was set to simulate the roasting process of FLMs. FLM solutions were immediately cooled in ice water to stop heat processing and then freeze-dried for subsequent analyses. FLMs prepared at different heating temperatures were termed FLM-37, FLM-55, FLM-70, FLM-100, and FLM-150, respectively. The FLM without heat treatment served as a control.

The retention rate of FLMs after simulating the heat-treated process was examined using a UPLC (Waters, USA) equipment ACQUITY UPLC ® BEH Shield RP 18 column (2.1 × 100 mm, 1.7 μm) and calculated as follows:

$$\text{Retention rate}(\%) = \frac{C_{\text{heat treated}}}{C_{\text{initial}}} \times 100 \quad (1)$$

where $C_{\text{heat treated}}$ is the concentration of FLMs after heat treatment and C_{initial} is the concentration of FLMs before heat treatment (5 mg mL^{-1}). A nonlinear gradient was performed using a two-buffer gradient system at a flow rate of 0.1 mL min^{-1}. The injection volume was 2 μL. The standard curve of FLMs was $y = 7762.2x - 368\,758$ (x: μg mL^{-1}, $r^2 = 0.996$). The selected gradient was consistent with the parameters described previously.[7,17]

2.4 Composition analysis of heat-treated FLM

According to our previous study,[7] the untreated and heat-treated FLM (2 mg mL^{-1}) were fully saponified in a 75 mM NaOH solution at 55 °C for 24 h. The reaction was terminated by adjusting the pH to 6.5–7.0 with 1 M HCl. The compositions of different FLM samples were examined by UPLC (Waters, USA). The standards employed for flaxseed lignan quantification include secoisolariciresinol diglucoside (SDG), herbacetin diglucoside (HDG), pinoresinol diglucoside (PDG), *p*-coumaric acid glycoside (CouAG), and ferulic acid glycoside (FerAG).

The freeze-dried FLM samples were employed for spectroscopy analysis using a TENSOR 27 Fourier transform infrared (FT-IR) spectrometer (Bruker) to analyze its structural properties. The spectra were recorded at a resolution of 4 cm^{-1} and a scan number of 32 in the range of 4000–700 cm^{-1} with air as the background at ambient temperature (25 °C).

2.5 Interfacial property of heat-treated/untreated FLMs

To simulate the realistic interfacial adsorption process of FLMs and S90 between flaxseed oil and water, the dynamic interfacial tension (γ) at the interface of FO and heat-treated/untreated FLM (0.03% w/w)-enriched aqueous phase was examined using a drop profile tensiometer (Tracker, Teclis Technologies, France). The droplet area was set to 15 mm^2 and the respective experiment was monitored at 25 °C for 3600 s. The drop profiles of γ were continuously monitored and then recorded as a function of time. The surface pressure was calculated using the following mathematical conversion relation (eqn (2)):[16]

$$\pi = \gamma_s - \gamma_p \quad (2)$$

where γ_s represents the surface tension of the oil/water solution and γ_p represents the surface tension of the oil/FLMs-S90 solution.

2.5.1 Langmuir–Blodgett film preparation. To further simulate the effect of FLMs on the structure of interface between oil and water, the Langmuir–Blodgett film was prepared using S90-FLM solutions. S90 solutions (2%, w/w) were mixed with untreated and heat-treated FLMs in a ratio of 1/10, while concentration of heat-treated/untreated FLMs was 0.5 mg mL^{-1} to form S90-FLM solutions. Langmuir-trough (KSV NIMA Liquid–Liquid, Finland, Sweden) was employed to prepare Langmuir–Blodgett films.[16] The FLM-enriched S90 dispersion liquid (100 μL) was injected and then spread on the water surface, while the interfacial pressure was monitored using a platinum William plate. The surface pressure was recorded as a function of water surface area.

The mica flakes were immersed in a trough with an ultrapure water aqueous phase and then pulled upwards (1 mm min^{-1}) at a certain surface pressure (20 mN m^{-1}). A freshly cut mica sheet (Highest Grade V1 Mica, Ted Pella, INC, USA) was used. The mica sheet with the film was reproduced and then dried in a desiccator for 2–3 days before observing through AFM (Bruker Dimension ICON, USA). Topographic measurements were performed using a ScanAsyst-Air model non-conducting tapered silicon nitride probe. The AFM images were analyzed and processed using Nanoscope Analysis software v1.5.

2.6 Antioxidant activity of heat-treated/untreated FLM

2.6.1 Total phenolic contents. The total phenolic contents were determined by the Folin–Ciocalteu colorimetric method with minor modifications.[17] In brief, FLMs (1 mg mL^{-1}) were mixed with the same volume of Folin–Ciocalteu phenol reagent. The mixture (0.2 mL) was incubated for 3 min, and 0.2 mL Na_2CO_3 solution was introduced. Then the mixture was diluted with distilled water to 2 mL. The total phenolic contents were examined using a UV/Visible spectrophotometer (DU 800, Beckman Coulter, Inc., USA) at 765 nm. The results are expressed in sinapic acid equivalents (SAE) per milliliter of the samples (mg SAE per mL, $y = 6.298x + 0.032$, $r^2 = 0.995$).

2.6.2 Ferric reducing antioxidant power (FRAP). The FRAP assay was performed according to previous study with minor

modifications.[17] In brief, 50 μL FLM solutions (1 mg mL^{-1}) were mixed with 100 μL FRAP reagent (2.5 mL of 0.1 M acetate buffer, pH 3.6, 2.5 mL of 10 mmol TPTZ in 40 mmol HCl, as well as 2.5 mL of 20 mmol $FeCl_3$) in a 2 mL centrifuge tube. Subsequently, the mixture was diluted with double-distilled water to 0.5 mL and incubated at 30 °C for 20 min. The absorbance was examined at 595 nm, and the results are expressed in milligram of sinapic acid equivalents (SAE) per milliliter of the samples (mg SAE per mL, $y = 78.176x + 0.133$, $r^2 = 0.998$).

2.6.3 ABTS and DPPH scavenging assay. The $ABTS^{\bullet+}$ stock solution was prepared by reacting 7.4 mM ABTS and 2.6 mM $K_2S_2O_8$ in equal amounts and then maintained in the darkness for 12 h. The working solution was prepared by diluting the stock solution with 10 mM phosphate buffer at pH 7.4 to 0.1 μmol mL^{-1}, and showed absorbance from 0.7 to 0.8 at 729 nm. FLMs (1 mg mL^{-1}) were mixed with 200 μL $ABTS^{\bullet+}$ in 1 : 10 proportion, and the absorbance of this mixture was recorded using a UV-vis spectrophotometer (Beckman Coulter Inc., USA) at 729 nm after 10 minutes of reaction.[17] The $ABTS^{\bullet+}$ scavenging capacity was determined by the percentage of inhibition as follows:

$$ABTS^{\bullet+}\ \text{scavenging rate}(\%) = \left(1 - \frac{A_s}{A_0}\right) \times 100 \quad (3)$$

where A_0 and A_s denoted the absorbance of the blank and sample, respectively. The concentration of $ABTS^{\bullet+}$ was determined to be 0.012 μmol $ABTS^{\bullet+}$/10 μL FLMs.

To maintain the same free radical concentration with $ABTS^{\bullet+}$, the DPPH working solution was diluted with methanol to 0.05 μmol mL^{-1} with the absorbance between 0.5 and 0.6 at 517 nm. Twenty microliters of FLMs (1 mg mL^{-1}) were mixed with 200 μL DPPH. After 30 min incubation, the absorbance of samples was recorded using a UV-vis spectrophotometer (Beckman Coulter Inc., USA) at 517 nm. The DPPH radical scavenging capacity was determined from the percentage of inhibition as follows:

$$\text{DPPH free radical scavenging rate}(\%) = \left(1 - \frac{A_s}{A_0}\right) \times 100 \quad (4)$$

where A_0 and A_s are the absorbances of the blank and sample, respectively. The concentration of DPPH radicals was determined to be 0.01 μmol/10 μL FLM.

2.7 Emulsion preparation

Emulsions were produced by high-speed homogenization followed by high-pressure microfluidics. The continuous phase was prepared by solubilizing 3% S90 and 0.5 mg mL^{-1} FLMs. Coarse FO emulsions were prepared by blending 20% FO (w/w) and 80% (w/w) aqueous phase using a high-speed blender (IKA, T25, Germany) at 10 000 rpm for 5 min. Fine FO emulsions were prepared using a microfluidizer (model M-110L, Microfluidics, Newton, MA) at 12 000 psi for four cycles.

2.8 Morphology of emulsions

The interfacial morphology of heat-treated/untreated FLM-enriched emulsion droplets was captured by cryo-scanning electron microscopy (Cryo-SEM, SU8010, Hitachi, Tokyo, Japan). Briefly, the emulsion (5.0–10.0 μL) was frozen in liquid nitrogen, transferred into a cryo-preparation chamber, cut into the cross-section at −90 °C and 1.3×10^{-6} mbar and then sputter-coated at 10 mA for 30 s. Finally, the samples were observed using a Cryo-SEM at 3 kV.

2.9 Analysis of physical and chemical stability during storage

FO emulsions with 0.02% (w/w) of sodium azide were packed into 10 mL glass tubes, sealed with a silicone plug and parafilm and then stored in the darkness at 37 °C for 3 weeks. The particle size and ζ-potential of FO emulsions were determined using a Mastersizer 3000 and a Nano-ZS, respectively. The microscopic morphology of FO emulsions was identified by confocal laser scanning microscopy (CLSM) (Nikon D-Eclipse C1 80i, Nikon, Melville, NY), and the CLSM images were processed using the Zen 2.6 software. The interface topography of FO emulsion droplets was observed by cryo-scanning electron microscopy (cryo-SEM) (SU8010, Hitachi, Japan).

The generation of primary oxidative products and secondary oxidative products of emulsions during storage was determined by a spectrophotometric method.[7] The values of hydroperoxides were expressed as mmol cumene hydroperoxide equivalents per kg of oil. The secondary oxidative products, malonaldehyde, were expressed as mmol 1,1,3,3-tetraethoxypropane (TEP) equivalents per kg of oil.

2.10 Statistical analysis

All assays were performed in triplicate, and the data are expressed as mean ± SD ($n = 3$). One-way ANOVA was performed to analyze the significant differences between data ($p < 0.05$) using SPSS 24 (SPSS Inc., Chicago, IL, USA). Principal component analysis (PCA) and partial least squares discriminant analysis (PLS-DA) were performed using MetaboAnalyst 5.0 (**https://www.metaboanalyst.ca**).

3. Results and discussion

3.1 Thermostability of FLM under different heating stresses

As shown in Fig. S1,† the purity of FLMs after extraction and purification was detected by UPLC at 280 nm, which reached 98%. Different heating processes were simulated for FLMs as digestion temperatures (37 °C, FLM-37), low-temperature sterilization temperatures (55 °C, FLM-55), pasteurization temperatures (70 °C, FLM-70), boiling temperatures (100 °C, FLM-100), and baking temperatures (150 °C, FLM-150). As shown in Fig. 1a, after treatment at 37 and 55 °C, there was no difference between the heat-treated FLMs and untreated FLMs. However, about 31%, 38%, and 52% of the FLM were degraded under higher temperature treatments (FLM-70, FLM-100, and FLM-150), respectively. As depicted in Fig. 1b, the heat-treated/untreated FLMs displayed typical absorption peaks of phenolic compounds, *i.e.*, the O–H and C–O stretching vibration of phenolic hydroxyl (Ar-OH), at 3369.36 and 1218 cm^{-1}. The C–H bending vibration of the methyl ($-CH_3$) groups was at

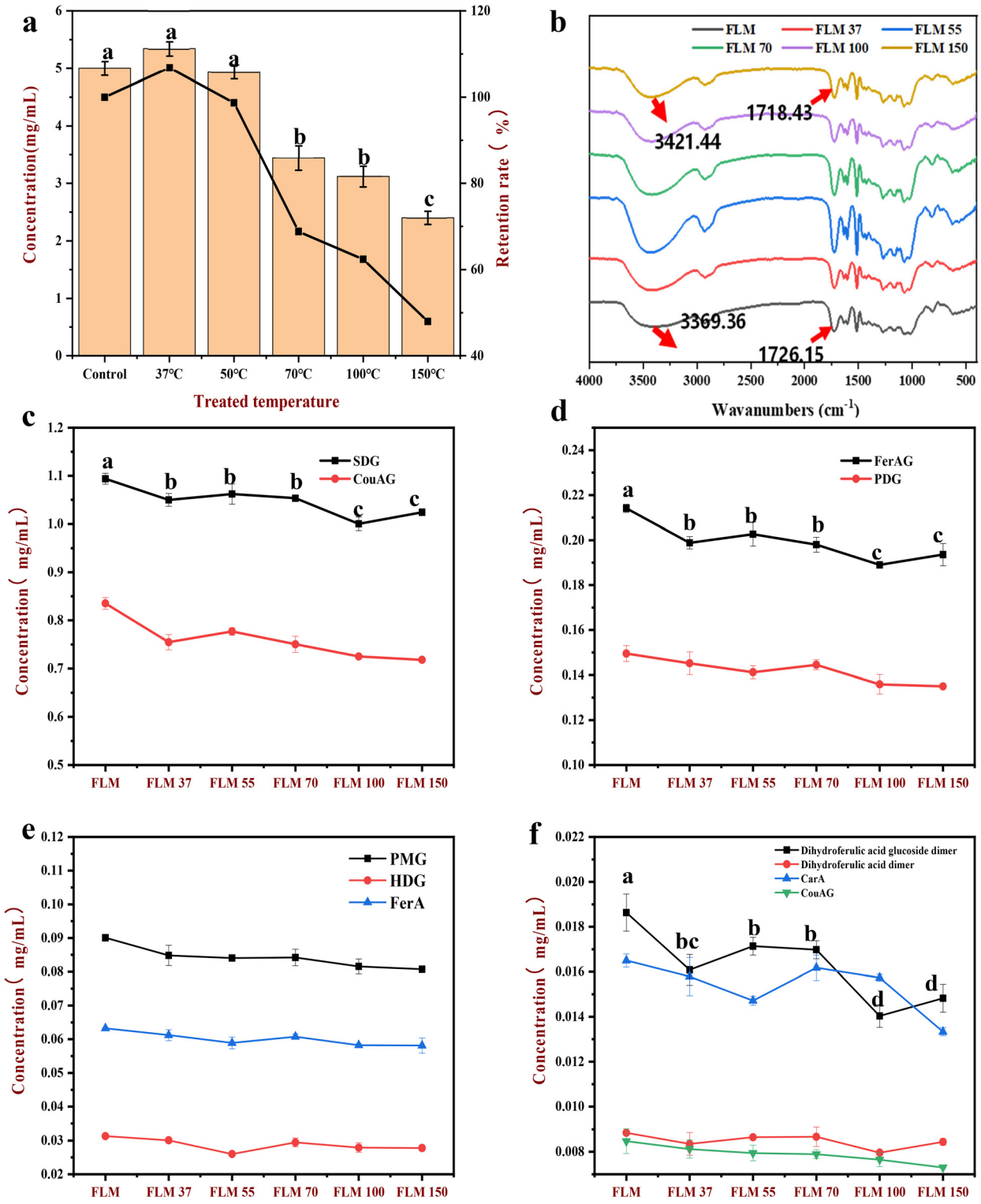

Fig. 1 (a) Retention rate of FLMs under different heat stresses. (b) Structural changes in FLMs after heat processing stresses (FT-IR); (c–f) composition changes in FLM before and after heat-treatment (UPLC). The data are expressed as mean ± SD (n = 3).

1458 cm^{-1}. The C═O stretching vibration of the FLM was identified at the wavenumber of 1900–1650 cm^{-1}. The C_{alkyl}–O stretching vibration of the methoxy (Ar-OCH_3) group was at 1120 cm^{-1}, and the C–H vibration of aromatic units was at 1600 cm^{-1} and 1510 cm^{-1}.[18–20] However, after high-temperature heat treatment, the O–H and C–O stretching vibration of FLM-70, FLM-100, and FLM-150 maximally shifted from 3369.36 cm^{-1} to 3421.44 cm^{-1}, and the C═O stretching

vibration maximally shifted from 1726 cm^{-1} to 1718.43 cm^{-1} compared with the FLM. This indicated that O–H was degraded, and formed quinone compounds after heating under 70 °C, 100 °C and 150 °C.

As shown in Fig. 1c–f, after complete hydrolysis, thirteen phenolic compounds were identified in the FLM, which comprised five lignans (+, −) SDG, PDG, and their monoglucoside (PMG) and aglycones, and four phenolic acids and their glucosides, namely, caffeic acid glucoside (CarfG), *p*-coumaric acid glucoside (CouAG), ferulic acid glucoside and its isomers ((E)-form/(Z)-form FerAG), and dihydroferulic acid dimers. Compared with FLM, the concentration of the composition in heat-treated FLM decreased under different thermal treatments. Besides, lignans and flavonoids in FLM-100 and FLM-150, such as SDG, PDG, and HDG, serving as the skeleton of FLMs, were slightly degraded (<1%). However, the concentration of phenolic acids at the end of the chain of FLM was decreased by 14% (CouAG), 10% (FerAG and its isomers), and 21% (dihydroferulic acid dimer), respectively ($p < 0.05$), which was consistent with the phenomena and conclusions reported in previous studies.[15]

The partial least squares discriminant analysis (PLS-DA) of the composition for heat-treated/untreated FLMs represented the disjoint union for FLM, FLM-100 and FLM-150, indicating the significant composition changes of FLMs under 100 and 150 °C heat treatment (Fig. 2). PLS-DA combined with the variable importance in projection (VIP) scores was adopted to select the phenolic compounds that significantly changed during heat treatment according to the criterion of VIP > 1. Dihydroferulic acid dimers such as FerA, (+, −) SDG, PDG, CouAG and (+, −) FerAG were regarded as characteristic compositions during heating with a higher VIP value (Fig. 2a). As shown in Fig. 2b, the cluster analysis had the same results as PLS-DA, which indicated that the phenolic compounds in FLM-100 and FLM-150 were significantly decreased compared with FLMs. Besides, phenolic acid glucuronides and flavonols such as FerAG, CouAG, and (+, −) SDG and PDG showed a significant positive correlation with heat treatment temperature.

FT-IR spectra indicated that the stretching vibration of compound hydroxyl appeared in the infrared wavenumber ranging from 3650 to 3500 cm^{-1}, which can be adapted to determine whether there exist phenols, acids, and alcohols in the compounds.[19] The FLM displayed characteristic peaks at wave numbers of 3369 cm^{-1}, 1726 cm^{-1} and 1458 cm^{-1}, suggesting the existence of hydroxyl, carbonyl, and benzene ring characteristic structures, respectively.[21] As revealed by the shift of O–H and C–O stretching vibrations for heat-treated FLMs, the phenolics were slightly decreased to aldehyde compounds. Besides, the ArO-H vibration signals of aromatic units were normalized to evaluate the relative contents of Ar-OH and C=O (ESI, Fig. S1†). As the treatment temperature of FLMs increases, the signal intensity of the O–H stretching vibration tended to be reduced, whereas the signal intensity of C=O increased, confirming the transformation of Ar-OH group into the C=O group. Therefore, it also indicated that the molecular structure of FLMs can be effectively reconstructed by heat-treatment, in particular phenolic-OH groups.[22] Those results indicated the good thermal stability of FLMs at lower temperatures such as the digestion temperature (37 °C) and sterilization temperature (55 °C) for 30 min. However, under higher temperature heat treatment (100 °C and 150 °C), the phenolic acids on the terminal of FLMs were easily degraded without the release of polyphenols, suggesting that the degradation of FLMs was limited and only existed in the oxidation of internal groups.[5]

At higher temperatures, the serious degradation of phenolic acids compared to lignans and flavonoids suggested that the degradation mainly occurred at the terminal of the chain of FLMs. However, the concentration of FerAG in FLM-150 was slightly higher than that of FLM-100 but without significance ($p > 0.05$), and this might be due to the isomerization between FerAG and its isomers or undifferentiated degradation of FerAG in FLMs under 100 °C and 150 °C.[23] As postulated in Fig. 3, the depolymerization, isomerization, and oxidation of FLMs may occur simultaneously when exposed to heat treatment.[24] Then, the oxidation of phenolic hydroxyl to form reactive semiquinone and quinone radicals can lead to the further formation of stabilized quinone structures.[25,26] Moreover, the isomerization of FerAG during thermal treatment has been demonstrated as a vital change, especially at higher processing temperatures.[11] Besides, the depolymerization of FLM may exist during heat processing and the release is relatively complex with a small molecular weight.[24,27]

3.2 Effect of heat treatment on the antioxidant activity of FLM

The total phenolic contents and FRAP of FLMs were measured to indicate the antioxidant activities of different mechanisms, *i.e.*, the transfer of electrons of phenolics.[28] SDG (0.1 mg mL^{-1}) and SECO (0.025 mg mL^{-1}) possessed the same number of hydroxyl groups with 1 mg mL^{-1} FLM ($M_w \approx 4641$, c(–OH) = 275 μmol L^{-1}) and were set as the control group. As indicated in Table 1, the total phenolic contents of SDG and SECO were 29.48 and 14.01 μg SA per mL, and the values of FRAP were 10.59 and 3.18 μg SA per mL, respectively. Besides, the $ABTS^{\bullet+}$ and $DPPH^{\bullet}$ free radical scavenging ability of SDG reached 76.17% and 63.07%, respectively, which was 66.7% and 50% higher than those of SECO ($p < 0.05$). For heat-treated/untreated FLMs, there were no obvious differences in the reducing power (FRAP), which was 40% lower than that of SDG but 50% higher than that of SECO ($p < 0.05$), respectively. Moreover, FLM-55 exhibited the highest total phenolic contents compared to other samples (34.51 ± 0.73 μg SA per mL, $p < 0.05$), which were 16.9% and 146% higher than those of SDG and SECO, respectively ($p < 0.05$). Moreover, for the ability to scavenge $DPPH^{\bullet}$ free radicals, there was no obvious difference between heat-treated/untreated FLMs (~85%), but 11.8% and 112% higher than those of SDG and SECO, respectively. Besides, FLM-150 exhibited the highest ABTS free radical scavenging ability (84.48 ± 2.87%, $p < 0.05$) compared to other samples, which was 34.1% and 310% higher than those of SDG and SECO ($p < 0.05$), respectively.

In theory, the total phenolic content is positively correlated with the antioxidant capacity of plant polyphenols, which also reflects the number of phenolic hydroxyl groups to a certain

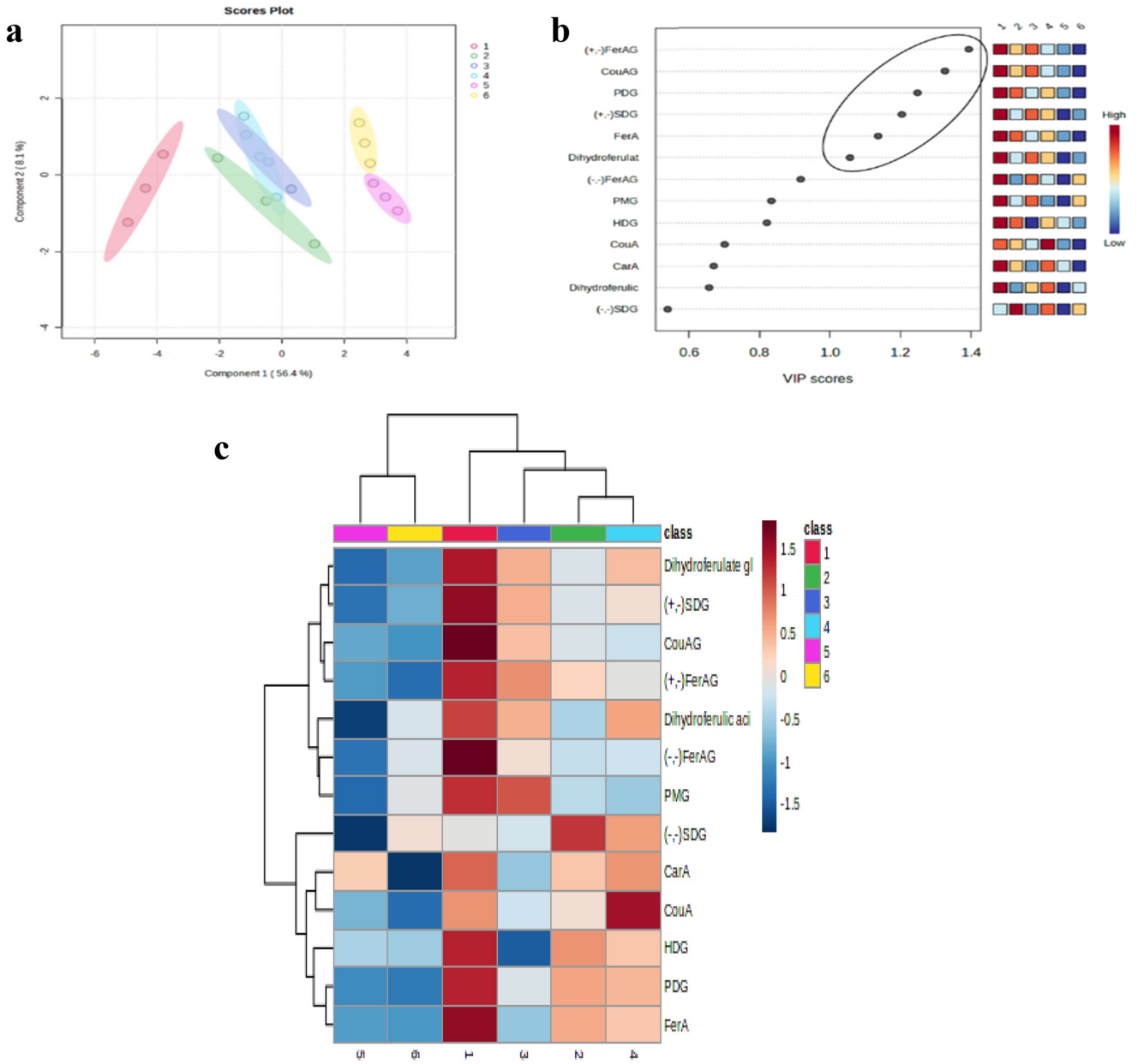

Fig. 2 Partial least squares discriminant analysis (PLS-DA) and cluster analysis of composition changes of FLMs before and after heat treatment: (a) PLS-DA score plot; (b) variable importance in projection (VIP) scores of each variable and cross-validation results; and (c) heatmap visualization of the changes in the composition of FLMs after heat treatment (class 1–6: FLM, FLM-37, FLM-55, FLM-70, FLM-100, and FLM-150).

extent.[29,30] As revealed by the above-mentioned results, the total phenolic contents of SDG were nearly two times higher than those of SECO at the identical concentration of hydroxyl groups, which was also in accordance with the number of hydroxyl groups in SDG and SECO. Therefore, FLMs had the same amount of total phenolic content with SDG, indicating no significant difference in the amount of phenolic hydroxyl groups among all samples. However, the DPPH and ABTS free radical scavenging capacity of heat-treated/untreated FLMs was slightly better than that of SDG at the identical concentration of hydroxyl groups. It was due to the higher antioxidant activity of flavonoids in the terminal of FLM chains such as HDG and PDG.[2] In general, at the same concentration of hydroxyl groups, HDG had a higher free radical scavenging capacity than that of SDG due to the *meta*-position dihydroxy moiety, which was an essential feature to evaluate the antioxidant activity.[31] Besides, due to the inconsistent antioxidant mechanisms, there was no significant difference between the results of FRAP with DPPH and ABTS-free radical scavenging activity for FLMs and SDG and SECO.[32] However, SDG had a higher value of FRAP than that of FLM due to the good water solubility, thus contributing to the transfer of a single electron in a polar reaction environment.[28] This suggested that the heat-treated/untreated FLM possessed a higher antioxidant activity

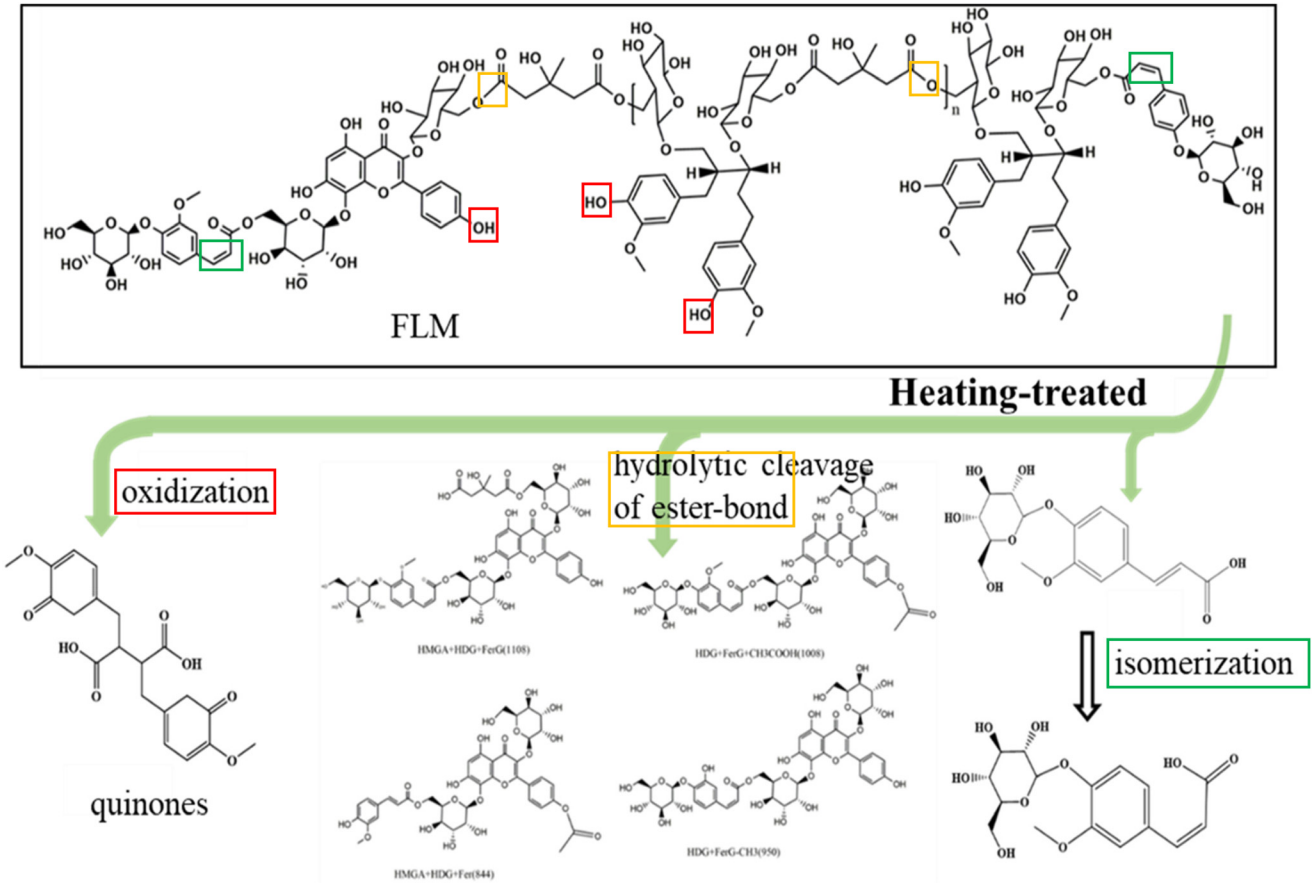

Fig. 3 Schematic of the structural changes of FLMs after heat treatment (ChemDraw Ultra 14.0). The reactive site and type are marked in red (oxidization), yellow (depolymerization) and green (isomerization).

Table 1 Antioxidant activities of heat-treated/untreated FLMs (DPPH and ABTS free radical scavenging ability, total phenol content and reducing capacity of ferrous ions); the data are expressed as mean ± SD (n = 3)

	Total phenolic (μg SA per mL)	FRAP (μg SA per mL)	DPPH free radicals scavenge (%)	ABTS free radicals scavenge (%)
FLM	31.44 ± 1.06 bc	6.00 ± 0.22 b	85.25 ± 0.35 a	81.37 ± 0.54 c
FLM-37	33.82 ± 0.09 b	5.47 ± 0.50 b	85.25 ± 0.25 a	81.47 ± 2.11 c
FLM-55	34.51 ± 0.73 ab	6.36 ± 0.37 b	83.97 ± 0.33 a	82.09 ± 0.65 bc
FLM-70	29.80 ± 0.84 bc	5.14 ± 0.29 b	84.54 ± 1.37 a	80.22 ± 2.34 c
FLM-100	30.28 ± 1.19 bc	6.23 ± 0.52 b	84.45 ± 0.21 a	79.79 ± 2.23 c
FLM-150	30.44 ± 2.18 bc	6.00 ± 0.45 b	84.89 ± 0.77 a	84.48 ± 2.87 a
SDG	29.48 ± 0.45 c	10.59 ± 0.35 a	76.17 ± 0.77 b	63.07 ± 2.31 d
SECO	14.01 ± 0.34 d	3.18 ± 0.15 c	40.14 ± 5.30 c	20.1 ± 0.34 e

than those of SDG and SECO at the identical concentration of hydroxyl groups. These results were in accordance with Kim *et al.*,[33] who confirmed that a simple heating process can be used as a tool to increase the antioxidant activity of grape seed extracts. Therefore, the FLM can serve as a more economic and efficient antioxidant than SDG and SECO.

As depicted in Fig. 1c–f, CouAG was seriously degraded by 12% after heat treatment under 150 °C. However, due to the weak antioxidant activity of CouAG, this change did not influence the antioxidant activity of FLMs.[34] Besides, after low-temperature heat treatment (37 °C and 55 °C), the total phenolic content of FLM was increased, suggesting the increased exposure of hydroxyl groups. It might be the depolymerization of FLMs under heat treatment due to the broken glycosidic bonds. Besides, after high-temperature heat treatment (70, 100, and 150 °C), the total phenolic content of FLMs declined due to the oxidation of phenolic hydroxyl groups.[35]

3.3 Effect of heat treatment on the interfacial adsorption behavior of FLMs

3.3.1 Interfacial pressure isotherms. It proved that polyphenols possessed amphipathy according to their phenolic

hydroxyl structure.[34,36,37] A complex molecular network consisting of FLMs and S90 at the air–water interface was investigated by the Langmuir–Blodgett technique to study the time-dependent adsorption of these materials and the formation of an S90-FLM film. The interfacial pressure isotherm curve of interfacial films formed by heat-treated/untreated FLMs at the air–water interface reflected the interfacial migration and adsorption behaviors. As depicted in Fig. 4a, when the interface area began to be compressed, the interfacial pressure for all groups increased, whereas it was maintained at 0 mN m^{-1} for the control. When the total area was narrowed to 150–300 cm^2, the interfacial pressure of heat-treated/untreated FLMs continued to decrease. The value of interfacial pressure of heat-treated/untreated FLMs was negatively correlated with heat-treated temperature. However, there were no significant correlations between interfacial pressure and heat-treated temperature of FLMs due to the intricate interplay of various factors, such as the composition and nature of the FLMs and the change in the composition and functional groups of FLM under different heat conditions. Besides, with the unit area further decreasing, the increased rate of the interfacial pressure of FLM-55 was decreased and finally reached the minimum interfacial pressure (~6.9 mN m^{-1}) compared with other samples (>8 mN m^{-1}). According to the adsorption dynamics and the compression isotherms, the behavior of heat-treated/untreated FLMs at the interface primarily falls into two stages.[38] First, the interfacial pressure increased immediately once heat-treated/untreated FLMs were added (stage I). During the process of stage I, the increased interfacial pressure indicated the rapid diffusion of heat-treated/untreated FLMs at the air–water interface and the formation of "fluid phase". Subsequently, as the interface was compressed, the interfacial pressure increased rapidly with the sharpest slope (stage II). During the process of stage II, the tiled FLMs came closer to each other and then formed the "condensed phase", suggesting the formation of dense interfacial films by FLMs. However, the structure and composition of FLMs were changed after heat treatment, which might influence the interfacial distribution of FLMs. As shown in Fig. 1, the O–H group in FLMs was degraded after heating under 70 °C, 100 °C and 150 °C, and accompanied by the thermal degradation of terminal phenolic acid glucuronides. Besides, the decreased number of hydrophilic phenolic hydroxyl groups might cause a variable amphiphilicity for different polyphenols and subsequently result in different interfacial distributions.[7] As a result, the lower surface pressure of FLM-55 than that of FLM-150 is due to the increasing content of phenolic hydroxyl groups, which promoted the interface extension of FLM-55 (Table 1, content of total phenolic). Therefore, the decreased hydrophilic property of FLMs might be more beneficial for their migration towards interface and further decreased the surface pressure between the water/air phase.[39]

An in-depth study was conducted to illustrate the effect of heat-treated/untreated FLMs on the compression isotherm curves of interfacial films formed by S90 during the interfacial adsorption. As depicted in Fig. 4b, the unit molecular area was nearly 41 Å when the surface pressure of S90 film reached the maximum (27.5 mN m^{-1}), suggesting "condensed phase" formation of S90 under that condition.[40] Besides, three stages for the behavior of heat-treated/untreated FLM-enriched S90 solutions are elucidated as follows: stage I: the zero-pressure stage is extremely low interfacial coverage, which was termed "gaseous phase"; stage II: with the interface compressing, the interfacial pressure of S90 is subjected to an initial increase, which was termed "fluid phase"; stage III, the tiled FLMs come closer with each other and then form the "condensed phase".[38] The emulsifier S90 began to form the "fluid phase" when the molecular area took up nearly 100 Å (Fig. 4b). After the addition of FLMs, the molecular area for "fluid phase" advanced to 125 Å, which was due to the higher molecular area of FLMs (MW > 4000) than S90 (MW ~768). Moreover, the surface pressure of the FLM-enriched S90 solution increased compared with that of S90, suggesting that competitive adsorption might exist between FLMs and S90 during co-absorption onto the interface. However, the potential noncovalent interactions between FLMs and S90 might lead to an undefined variation tendency of surface pressure of FLM-enriched S90 solutions.

To further investigate the microstructure of heat-treated/untreated FLM-enriched S90 films, the LB films were prepared on the mica flakes when the surface pressure was under 20 mN m^{-1}. Furthermore, the mica flakes were observed by atomic force microscopy (AFM). As presented in Fig. 4e, the films formed by S90 were continuous and without any defect due to the excellent interfacial properties of phospholipids. Under the scale of 3 μm, the images indicated that FLM, FLM-37, and FLM-55 did not affect the dispersibility and compactness of S90 films, while FLM-70, FLM-100, and FLM-150 led to the depression formation on S90 films. Under the scale of 0.5 μm, the images showed obvious defects for all FLM-enriched S90 films, especially for FLM-37, FLM-55, and FLM-70. Besides, FLM-enriched S90 (except for FLM-55) films showed obvious depression under the surface pressure at 20 mN m^{-1}. However, FLM-55-enriched S90 collapsed since the pressure approached the critical pressure (22 mN m^{-1}). FLM-150-enriched S90 formed relatively intact films for their prominent interfacial property. Therefore, for heat-treated/untreated FLMs, FLM-150 exhibited a higher increased rate of interfacial pressure than other samples, suggesting that the dense film may be formed.

3.3.2 Interfacial properties. The adsorption dynamics of S90 on the FO-water interface was examined to gain more insights into the effect of heat-treated/untreated FLMs on the interfacial behavior of emulsifier S90. The lower interfacial tension indicated that less energy was needed to break up the lipid droplets and form emulsions. As shown in Fig. 4c, the interfacial tension decreased rapidly from 12.7 mN m^{-1} to 6.5–7.5 mN m^{-1} in all groups, among which emulsifier S90 largely decreased the interfacial tension of the FO-water interface to 6.5 mN m^{-1} (control). However, the addition of heat-treated/untreated FLMs led to a slightly increased interfacial tension of FO-water interface, especially for FLM-100 and

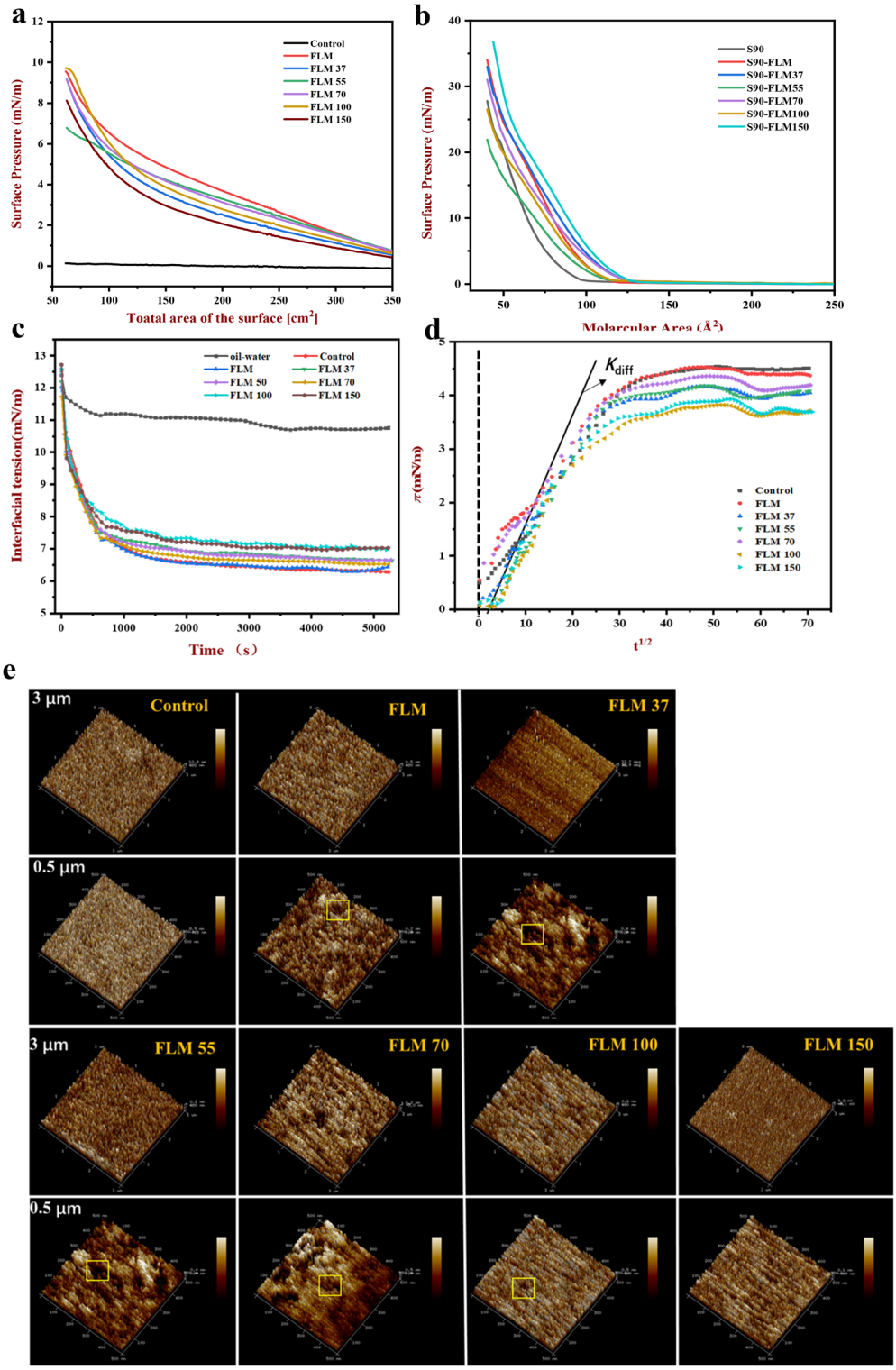

Fig. 4 (a) Surface pressure as a function of the total area of the surface for FLM before and after heat treatment; the surface pressure of methanol was set as the control group. (b) Surface pressure as a function of molecular area for S90 with the FLM before and after heat treatment. The surface pressure of S90 solution was set as the control. (c and d) Interfacial pressure as a function of time for S90 with the FLM before and after heat treatment at the oil/water interface (K_{diff} quantifies the diffusion rate), the interfacial pressure between oil and S90 solution was set as the control. (e) AFM images of Langmuir–Blodgett films made from S90 with the FLM before and after heat treatment. The data are expressed as mean ± SD (n = 3).

FLM-150. As depicted in Fig. 4d, the interfacial pressure π was converted as $\gamma_{sample} - \gamma_{control}$ and the time t was plotted as a function of $t^{1/2}$. At the initial adsorption process, a plot of π against $t^{1/2}$ would be linear and the slope of this plot of the diffusion rate was constant (K_{diff}), which was used to quantify the diffusion rate.[41] The K_{diff} value of emulsifier S90 (control group) was 0.103 (LR: 0.94), and the adsorption behaviors were similar to FLM, FLM-37, FLM-55 and FLM-70-enriched S90

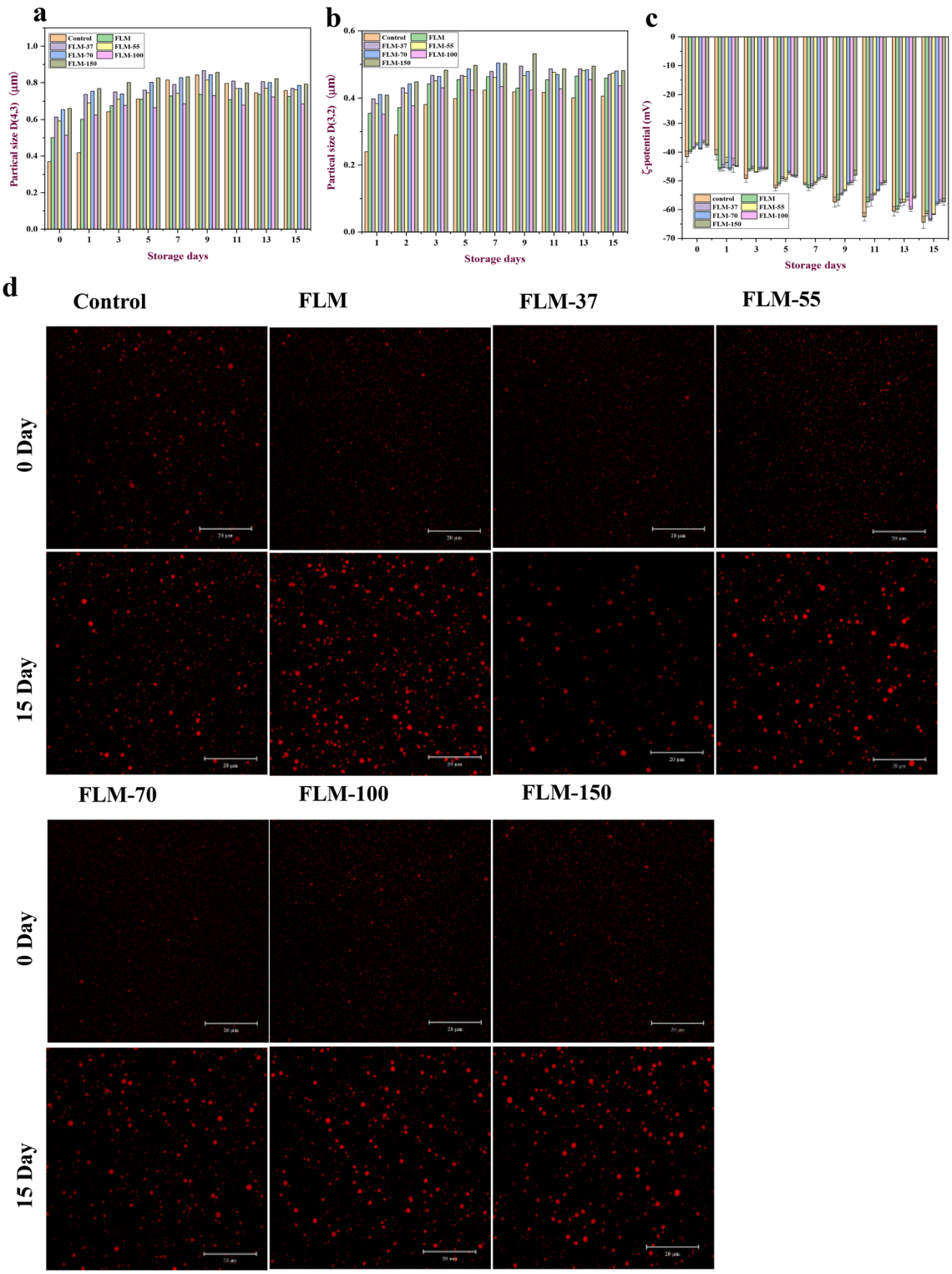

Fig. 5 Stability of S90-stabilized emulsion during storage. (a–c) Particle size and potential; the data are expressed as mean ± SD (n = 3). (d) The morphology observations of emulsions (confocal laser scanning microscopy).

solutions due to the insignificant difference for K_{diff}. Nevertheless, FLM-100 and FLM-150 exhibited higher K_{diff} values (~0.158 and 0.1758, LR: 0.93), suggesting a faster adsorption rate of FLM-100 and FLM-150 than that of other samples.[42] Therefore, as indicated by the results of interfacial adsorption kinetics, heat-treated/untreated FLMs inhibited the interfacial adsorption of S90, which was due to the competitive adsorption of FLMs with S90. Existing research has also indicated that the interfacial pressure π showed a linear relationship with $t_{1/2}$, suggesting that the interfacial adsorption process of S90 to the oil–water interface is diffusion-controlled by FLMs at the initial stage.[43] Besides, higher temperature-treated FLM can positively affect the interfacial properties of S90, which was correlated with the higher amphiphilicity of heat-treated FLMs.[44]

3.4 Effect of heat-treated FLM on the stability of FO emulsions

3.4.1 Physical stability. According to interfacial antioxidant theory, the higher antioxidant activity and interfacial properties of heat-treated/untreated FLMs indicated that they might have superior applications in emulsion systems.[45] The S90-stabilized FO emulsion was prepared *via* high-pressure microfluidization to examine the antioxidant potential of heat-treated FLMs. As depicted in Fig. 5a and b, initially, the mean particle size of S90-stabilized emulsion was approximately 0.369 and 0.24 μm for $D(4,3)$ and $D(3,2)$, while the mean particle size of FLM-enriched S90-stabilized emulsion droplets was more than 0.5 and 0.3 μm. During the storage, the particle sizes ($D(4,3)$) of all emulsions were increased to ~800 nm after storage, which was largely increased from 369 nm to 754 nm (>100%) for S90-stabilized emulsions ($p < 0.05$). For heat-treated/untreated FLM-enriched S90-stabilized emulsions, the particle size diameter increased by 18–40% after 15 days of storage, among which higher temperature-treated FLMs inhibited the increase in particle size diameter. For FLM-150-enriched S90 stabilized emulsions, the particle size diameter only increased by 18% after storage. Fig. 5c indicates that the S90-stabilized emulsion droplets had a relatively high negative surface charge (approximately −42 mV). The negative surface charge of FLM-enriched S90-stabilized emulsion droplets was slightly decreased to approximately −36 to −39 mV. These results suggested that all heat-treated/untreated FLMs contributed positive charges to the S90-rich interfacial layers, which might occur because of the replacement of some S90 by FLMs. Moreover, the absolute ζ-potential of all emulsions increased during the whole storage, which was due to the interfacial adsorption of lipid oxidation products.

As revealed by the macroscopic evaluation of emulsions, all emulsions were kept stable during the storage with no leakages of either oil or water phases or aggregation of droplets. The microspheres with an average diameter of nearly 400 nm for S90-stabilized emulsion were observed from the SEM images (Fig. 6b). In contrast, the average diameter of FLM-enriched emulsions was larger than that of S90-stabilized

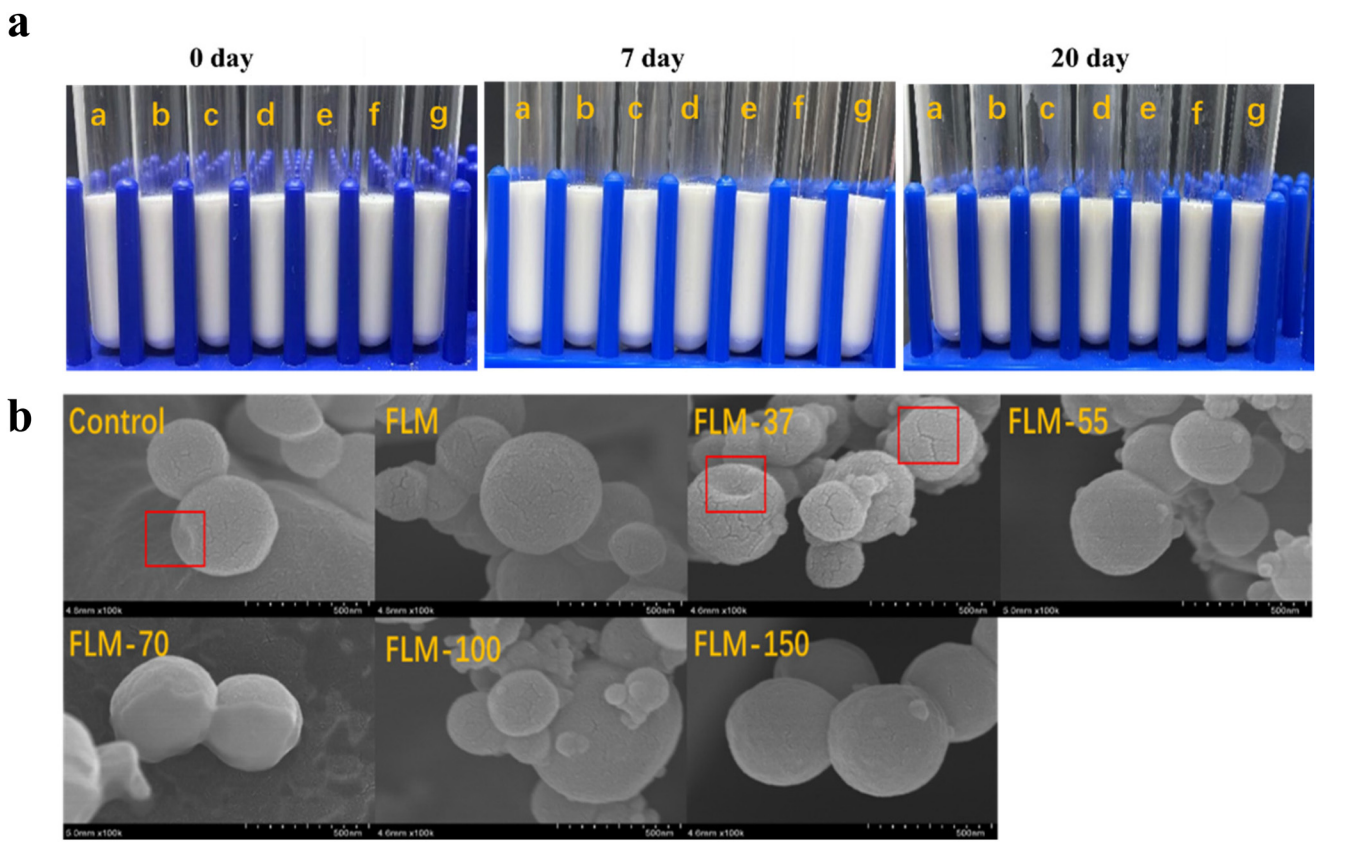

Fig. 6 (a) Appearance of emulsions (0, 7 and 20 d), (letters a–g represent FLM, FLM-37, FLM-55, FLM-70, FLM-100, and FLM-150). (b) The morphology observations of emulsions using cryo-scanning electron microscopy (0 d).

emulsions, and their surface was micro-concave with densely distributed shallow craquelure. Moreover, the observed results of particle size by SEM were consistent with the $D(4,3)$. Notably, FLM-150 enriched emulsions exhibited a much smoother surface, and their particle size was evenly distributed (Fig. 6b). Furthermore, as depicted in Fig. 5d, all CLSM images showed very fine lipid droplets (red) evenly distributed in the aqueous phase (black) at the initial stage. Similar to the results of $D(4,3)$, the size of the lipid particles increased after storage.

Moreover, $D(3,2)$ has been extensively employed to evaluate the droplet size of freshly prepared emulsions.[46] Besides, $D(4,3)$ has been often adopted to monitor the droplet size changes of the emulsion during storage.[47] The results of $D(3,2)$ suggested that the addition of FLMs led to 32%–79% increase in the particle size of S90-stabilized emulsions due to the bridged effect between FLMs and S90.[48,49] The change in CLSM images and $D(4,3)$ during storage indicated a positive effect on the physical stability of S90-stabilized emulsions by all types of FLMs, especially for FLM-150. The compression isotherm curves further illustrated that the thicker and higher viscoelastic interfacial film formed in FLM-150-enriched S90. Besides, Fig. 4c further revealed the decreased emulsion stability of S90 by FLMs due to the interactions between them. For heat-treated/untreated FLMs, the value of interfacial tension between FLM-150-enriched S90 solution and FO was maximum, which showed the largest particle size after emulsification to form an emulsion. Furthermore, FLMs could also interact with phospholipids *via* hydrogen bond and hydrophobic interactions, which were mainly determined by the polyphenol's polarity. Due to the weak polarity of FLMs, they were expected to interact with the nonpolar acyl chain region deep of phospholipids and this depth decreased with the increase in polarity.[50] Therefore, the different polarity of heat-treated FLMs further influenced their interface positioning and stability of emulsions.

3.4.2 Chemical stability. The S90-stabilized FO emulsion was unstable and easy to be oxidized due to the high proportion of PUFAs in FO (>50%) as well as their high oxidative susceptibility. As shown in Fig. 7a–d, lipid hydroperoxides and

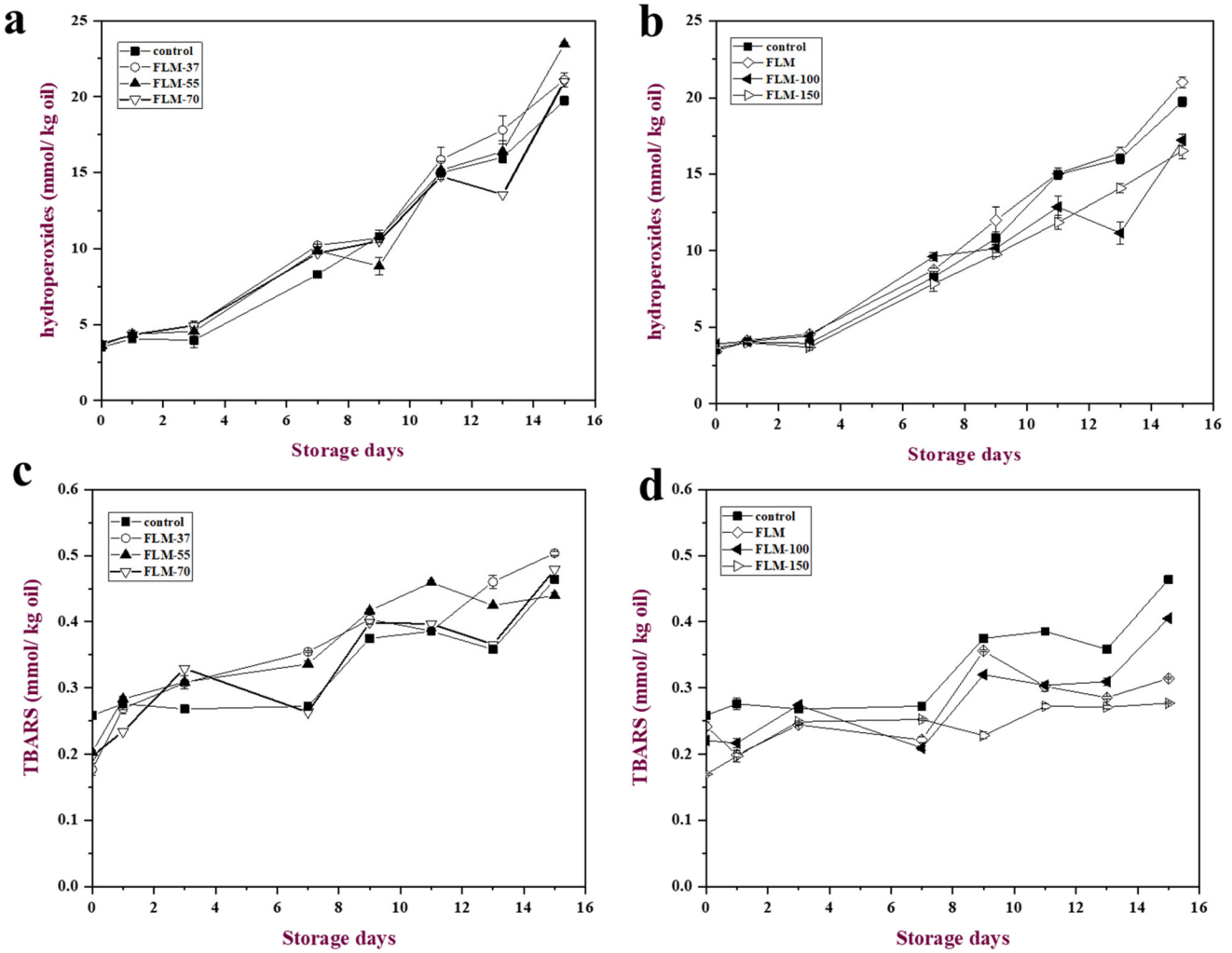

Fig. 7 Hydroperoxide (a and b) and malonaldehyde (c and d) formation in FO emulsions containing different types of lignans (FLM, FLM-37, FLM-55, FLM-75, FLM-100 and FLM-150) during storage.

TBARS concentrations in all of the samples were at identical levels initially. Subsequently, all the emulsions exhibited a lag phase in the first three days of storage, followed by a steep rise in the generation of primary reaction products (Fig. 7a and b). Besides, during the storage, the addition of FLM, FLM-37, FLM-55 and FLM-70 did not significantly affect the generation of lipid hydroperoxides (Fig. 7a) and TBARS (Fig. 7c). However, compared with S90 stabilized emulsion, the concentration of hydroperoxides was reduced by 26.7% in FLM-100 and FLM-150, whereas the concentration of TBARS maximally declined by 80% ($p < 0.05$) (Fig. 7b and d). The results indicated that FLM-100 and FLM-150 had the ability to inhibit lipid oxidation in S90-stabilized emulsions, particularly the secondary oxidative product formation.

According to previous study, the antioxidant activity of plant polyphenols generally reduced after high-temperature heat treatments (*e.g.*, tea polyphenols and grape seed extract).[24,35] However, the antioxidant activity of FLMs was improved after heat treatment, which might be due to the prominent stability of FLMs against heat treatment attributed to its relatively highly stable ester-bonded oligomer structure compared with those plant polyphenolics. Accordingly, when treated at high temperatures (100 and 150 °C), the FLM depolymerized and released monomers and other lower oligomers, which increased its antioxidant activity.[51] Notably, all heat-treated/untreated FLMs were proved to possess interfacial properties, especially for FLM-100 and FLM-150, suggesting the possible higher adsorption contents of FLM-100 and FLM-150 than FLM, FLM-37, FLM-55 and FLM-70. The better interfacial anchoring of FLM-100 and FLM-150 further increased their interfacial antioxidant effect. Besides, FLM-100 and FLM-150-enriched S90 formed a thick and dense interfacial film, which can inhibit the attack of prooxidative factors for lipids. However, there was no significant difference in the antioxidant capability between low-temperature-treated FLMs in emulsions, which might be because (i) no significant changes in the FLM structure at low temperatures, (ii) no depolymerization of FLM occurred at low temperatures, which further kept higher lipophilicity and were likely to be embedded deeply into the phospholipid molecule, hindering their interfacial antioxidant reactions and even reducing interfacial density, (iii) the un-depolymerized FLMs exhibited higher steric hindrance on the interface of emulsion droplets, which were likely to interfere with the radical scavenging capacity exhibited by the phenol hydroxyl group.

4. Conclusion

In this study, the chemical composition and antioxidant activity of FLMs under different thermal processes were examined. The results indicated that all heat-treated and untreated FLMs had superior antioxidant activity to their structural units SDG and SECO at the same hydroxyl concentration. This was attributed to the higher antioxidant activity of flavonoids located at the terminal of the FLM chain, such as HDG and PDG. Although the phenolic acids at the end of the FLM chain were significantly reduced, this did not affect their antioxidant activity. Furthermore, we systematically explored the relationship between the structural changes of FLMs under different heat processes and their effects on the physicochemical stability of emulsions. The results indicated that the FLM and its low-temperature-treated products (FLM-37, FLM-55, and FLM-70) exhibited limited antioxidant activity in S90-stabilized FO emulsions, due to the limited interfacial properties of their intact and large molecular structures. In contrast, FLM-100 and FLM-150 demonstrated higher antioxidant activity and interfacial properties, further enhancing the physicochemical stability of the S90-stabilized FO emulsion system. Therefore, the interfacial anchoring of FLMs primarily contributed to their higher interfacial antioxidant activity in emulsions. In conclusion, FLM-100 and FLM-150 were identified as excellent antioxidants for PUFA-enriched emulsions, owing to their outstanding interfacial properties and antioxidant activity. Our findings are also expected to offer a novel and environmentally friendly strategy for promoting the widespread use of natural polymerized plant polyphenols as antioxidants in the food industry.

Abbreviations

FLM	Flaxseed lignan macromolecules
DFHP	Defatted flaxseed hull powder
S90	Sunflower lecithin Sunlipon™ 90
SDG	Secoisolariciresinol diglucoside
SECO	Secoisolariciresinol
HDG	Herbacetin diglucoside
PDG	Pinoresinol diglucoside
CouAG	*p*-Coumaric acid glycoside
FerAG	Ferulic acid glycoside
FO	Flaxseed oil
ALA	α-Linolenic acid
EPA	Eicosapentaenoic
DHA	Docosahexaenoic
TBA	2-Thiobarbituric acid
CLSM	Confocal laser scanning microscopy
DPPH	2,2-Diphenyl-1-picrylhydrazyl
TCA	Trichloroacetic acid
TEP	1,1,3,3-Tetraethoxypropane
AAPH	2,2-Azobis-2-methylpropanimidamide dihydrochloride
FRAP	Ferric reducing antioxidant power
SAE	Sinapic acid equivalents

Author contributions

Chen Cheng: investigation, formal analysis, writing – original draft preparation and review & editing; Xiao Yu: development or design of methodology, writing – review & editing preparation; Fenghong Huang: data curation and supervision; Lei

Wang: investigation and formal analysis; Zhenzhou Zhu: methodology, development or design of methodology and creation of models; Jing Yang: writing – critical review, commentary and revision; Peng Chen: methodology; Qianchun Deng: resources; conceptualization, ideas; formulation or evolution of overarching research goals and aims; funding acquisition, acquisition of the financial support for the project leading to this publication.

Data availability

The data for this article are available at Web of Science at **https://doi.org/10.1039/d4fo02663b**. Besides, the data supporting this article have been included as part of the ESI.†

Conflicts of interest

There are no conflicts to declare.

Acknowledgements

The authors gratefully acknowledge the financial support from the National Natural Science Foundation of China (32072267) and supported by the Earmarked Fund for China Agriculture Research System (CRAS-14).

References

1 L. X. Wang, H. L. Wang, J. Huang, T. Z. Chu, C. Peng, H. Zhang, H. L. Chen, Y. A. Xiong and Y. Z. Tan, Review of lignans from 2019 to 2021: Newly reported compounds, diverse activities, structure-activity relationships and clinical applications, *Phytochemistry*, 2022, **202**, 113326.

2 T. J. Tse, Y. Guo, Y. Y. Shim, S. K. Purdy, J. H. Kim, J. Y. Cho, J. Alcorn and M. J. T. Reaney, Availability of bioactive flax lignan from foods and supplements, *Crit. Rev. Food Sci. Nutr.*, 2022, 1–16.

3 Health Canada 2014. Summary of health Canada's assessment of a health claim about ground whole flaxseed and blood cholesterol lowering. Accessed September 17, 2021. **https://www.canada.ca/content/dam/hc-sc/migration/hc-sc/fn-an/alt_formats/pdf/label-etiquet/claims-reclam/assess-evalu/flaxseed-graines-de-lin-eng.pdf**.

4 J. L. Adolphe, S. J. Whiting, B. H. J. Juurlink, L. U. Thorpe and J. Alcorn, Health effects with consumption of the flax lignan secoisolariciresinol diglucoside, *Br. J. Nutr.*, 2010, **103**(07), 929–938.

5 A. Mueed, M. Ibrahim, S. Shibli, P. Madjirebaye, Z. Deng and M. Jahangir, The fate of flaxseed-lignans after oral administration: a comprehensive review on its bioavailability, pharmacokinetics, and food design strategies for optimal application, *Crit. Rev. Food Sci. Nutr.*, 2022, 1–19.

6 S. Rahmawaty and B. J. Meyer, Stunting is a recognized problem: Evidence for the potential benefits of omega-3 long-chain polyunsaturated fatty acids, *Nutrition*, 2020, **73**, 110564.

7 C. Cheng, X. Yu, F. Huang, D. Peng, H. Chen, Y. Chen, Q. Huang and Q. Deng, Effect of different structural flaxseed lignans on the stability of flaxseed oil-in-water emulsion: An interfacial perspective, *Food Chem.*, 2021, **357**, 129522.

8 L. Couedelo, S. Amara, M. Lecomte, E. Meugnier, J. Monteil, L. Fonseca, *et al.*, Impact of various emulsifiers on ALA bioavailability and chylomicron synthesis through changes in gastrointestinal lipolysis, *Food Funct.*, 2015, **6**(5), 1726–1735.

9 S. Trattner, B. Ruyter, T. K. Østbye, T. Gjøen, V. Zlabek, A. Kamal-Eldin, *et al.*, Sesamin increases alpha-linolenic acid conversion to docosahexaenoic acid in atlantic salmon (salmo salar l.) hepatocytes: role of altered gene expression, *Lipids*, 2008, **43**(11), 999–1008.

10 O. Pabois, C. D. Lorenz, R. D. Harvey, I. Grillo, M. M. Grundy, P. J. Wilde, *et al.*, Molecular insights into the behaviour of bile salts at interfaces: A key to their role in lipid digestion, *J. Colloid Interface Sci.*, 2019, **556**, 266–277.

11 H. Debelo, M. Li and M. G. Ferruzzi, Processing influences on food polyphenol profiles and biological activity, *Curr. Opin. Food Sci.*, 2020, **32**, 90–102.

12 Y. Chen, H. Lin, M. Lin, P. Lin and J. Chen, Effects of thermal preparation and in vitro digestion on lignan profiles and antioxidant activity in defatted-sesame meal, *Food Chem. Toxicol.*, 2019, **128**, 89–96.

13 H. K. Hyvärinen, J. M. Pihlava, J. A. Hiidenhovi, V. Hietaniemi, H. J. T. Korhonen and E. L. Ryhänen, Effect of processing and storage on the stability of flaxseed lignan added to bakery products, *J. Agric. Food Chem.*, 2006, **54**(1), 48–53.

14 X. Yang, Y. Guo, T. J. Tse, S. K. Purdy, R. Mustafa, J. Shen, J. Alcorn and M. J. T. Reaney, Oral pharmacokinetics of enriched secoisolariciresinol diglucoside and its polymer in rats, *J. Nat. Prod.*, 2021, **84**(6), 1816–1822.

15 E. Gerstenmeyer, S. Reimer, E. Berghofer, H. Schwartz and G. Sontag, Effect of thermal heating on some lignans in flax seeds, sesame seeds and rye, *Food Chem.*, 2013, **138**(2), 1847–1855.

16 J. Yang, Y. Duan, H. Zhang, F. Huang, C. Wan, C. Cheng, L. Wang, D. Peng and Q. Deng, Ultrasound coupled with weak alkali cycling-induced exchange of free sulfhydryl-disulfide bond for remodeling interfacial flexibility of flaxseed protein isolates, *Food Hydrocolloids*, 2023, 140.

17 C. Cheng, K. Yu, X. Yu, F. Geng, F. Huang, L. Wang, Q. Huang, S. Quan and Q. Deng, Optimized endogenous lipid concomitants in flaxseed oil by different oil extraction technologies: Their positive roles in emulsions, *LWT – Food Sci. Technol.*, 2022, 155.

18 J. S. Rodrigues, A. d. S. M. de Freitas, C. C. Maciel, S. F. Mendes, D. Diment, M. Balakshin and V. R. Botaro,

Selection of kraft lignin fractions as a partial substitute for phenol in synthesis of phenolic resins: Structure-property correlation, *Ind. Crops Prod.*, 2023, 191.

19 C. Wen, D. Song, L. Zhuang, G. Liu, L. Liang, J. Zhang, X. Liu, Y. Li and X. Xu, Isolation and identification of polyphenol monomers from celery leaves and their structure-antioxidant activity relationship, *Process Biochem.*, 2022, **121**, 69–77.

20 G. Zhu, D. Ye, X. Chen, Y. Wu, Z. Yang, Y. Mai, B. Liao and J. Chen, Lignin-derived polyphenols with enhanced antioxidant activities by chemical demethylation and their structure-activity relationship, *Int. J. Biol. Macromol.*, 2023, **237**, 124030.

21 M. A. Hossain and S. M. Mizanur Rahman, Isolation and characterisation of flavonoids from the leaves of medicinal plant Orthosiphon stamineus, *Arabian J. Chem.*, 2015, **8**(2), 218–221.

22 A. Majira, B. Godon, L. Foulon, J. C. van der Putten, L. Cezard, M. Thierry, F. Pion, A. Bado-Nilles, P. Pandard, T. Jayabalan, V. Aguie-Beghin, P. H. Ducrot, C. Lapierre, G. Marlair, R. J. A. Gosselink, S. Baumberger and B. Cottyn, Enhancing the Antioxidant Activity of Technical Lignins by Combining Solvent Fractionation and Ionic-Liquid Treatment, *ChemSusChem*, 2019, **12**(21), 4799–4809.

23 C. Arruda, V. Pena Ribeiro, M. Oliveira Almeida, J. A. Aldana Mejia, R. Casoti and J. Kenupp Bastos, Effect of light, oxygen and temperature on the stability of artepillin C and p-coumaric acid from Brazilian green propolis, *J. Pharm. Biomed. Anal.*, 2020, **178**, 112922.

24 S. Chamorro, I. Goñi, A. Viveros, D. Hervert-Hernández and A. Brenes, Changes in polyphenolic content and antioxidant activity after thermal treatments of grape seed extract and grape pomace, *Eur. Food Res. Technol.*, 2011, **234**(1), 147–155.

25 M. Y. Coseteng and C. Y. Lee, Changes in Apple Polyphenoloxidase and Polyphenol Concentrations in Relation to Degree of Browning, *J. Food Sci.*, 2010, **52**(4), 985–989.

26 L. Pourcel, J. M. Routaboul, V. Cheynier, L. Lepiniec and I. Debeaujon, Flavonoid oxidation in plants: From biochemical properties to physiological functions, *Trends Plant Sci.*, 2007, **12**(1), 29–36.

27 M. J. Gonzalez, J. L. Torres and I. Medina, Impact of thermal processing on the activity of gallotannins and condensed tannins from hamamelis virginiana used as functional ingredients in seafood, *J. Agric. Food Chem.*, 2010, **58**(7), 4274–4283.

28 J. Rumpf, R. Burger and M. Schulze, Statistical evaluation of DPPH, ABTS, FRAP, and Folin-Ciocalteu assays to assess the antioxidant capacity of lignins, *Int. J. Biol. Macromol.*, 2023, **233**, 123470.

29 Y. Guo, S. Shi, N. Yang, M. X. Tang, Z. J. Duan, X. R. Guo and Z. H. Tang, Comparative assessment of nutritional composition, polyphenol profile and antioxidative properties of wild edible ferns from northeastern China, *Food Res. Int.*, 2023, **163**, 112237.

30 C. Y. Woumbo, D. Kuate and H. M. Womeni, Cooking methods affect phytochemical composition and anti-obesity potential of soybean (Glycine max) seeds in Wistar rats, *Heliyon*, 2017, **3**(8), e00382.

31 R. Praveena, K. Sadasivam, V. Deepha and R. Sivakumar, Antioxidant potential of orientin: A combined experimental and DFT approach, *J. Mol. Struct.*, 2014, **1061**, 114–123.

32 R. L. Prior, X. Wu and K. Schaich, Standardized methods for the determination of antioxidant capacity and phenolics in foods and dietary supplements, *J. Agric. Food Chem.*, 2005, **53**(10), 4290–4302.

33 S. Y. Kim, S. M. Jeong, W. P. Park, K. C. Nam, D. U. Ahn and S. C. Lee, Effect of heating conditions of grape seeds on the antioxidant activity of grape seed extracts, *Food Chem.*, 2006, **97**(3), 472–479.

34 C. Cheng, X. Yu, D. J. Mcclements, Q. D. Huang, H. Tang, K. Yu, X. Xiang, P. Chen, X. T. Wang and Q. C. Deng, Effect of flaxseed polyphenols on physical stability and oxidative stability of flaxseed oil-in-water nanoemulsions, *Food Chem.*, 2019, **301**, 125207.

35 Z. Jiang, Z. Han, M. Zhu, X. Wan and L. Zhang, Effects of thermal processing on transformation of polyphenols and flavor quality, *Curr. Opin. Food Sci.*, 2023, 51.

36 V. Aguie-BeGhin, P. Sausse, E. Meudec, V. Cheynier and R. Douillard, Polyphenol β-Casein Complexes at the Air/Water Interface and in Solution: Effects of Polyphenol Structure, *J. Agric. Food Chem.*, 2008, **56**(20), 9600–9611.

37 G. Fabre, I. Bayach, K. Berka, M. Paloncyova, M. Starok, C. Rossi, J. L. Duroux, M. Otyepka and P. Trouillas, Synergism of antioxidant action of vitamins E, C and quercetin is related to formation of molecular associations in biomembranes, *Chem. Commun.*, 2015, **51**(36), 7713–7716.

38 F. Sun, Q. Wang, C. Gao, H. Xiao and N. Yang, Effect of extraction pH and post-extraction heat treatment on the composition and interfacial properties of peanut oil bodies, *Colloids Surf., A*, 2023, 656.

39 A. Mohammadi, P. A. Kashi, M. Kashiri, A. Bagheri, J. Chen, R. Ettelaie, H. Jäger and M. Shahbaz, Self-assembly of plant polyphenols-grafted soy proteins to manufacture a highly stable antioxidative pickering emulsion gel for direct-ink-write 3d printing, *Food Hydrocolloids*, 2023, **142**, 108851.

40 A. S. Girard-Egrot, S. P. Godoy and L. C. Blum, Enzyme association with lipidic Langmuir–Blodgett films: Interests and applications in nanobioscience, *Adv. Colloid Interface Sci.*, 2005, **116**, 205–225.

41 X. Feng, H. Dai, L. Ma, Y. Fu, Y. Yu, H. Zhou, T. Guo, H. Zhu, H. Wang and Y. Zhang, Properties of Pickering emulsion stabilized by food-grade gelatin nanoparticles: influence of the nanoparticles concentration, *Colloids Surf., B*, 2020, **196**, 111294.

42 W. Xiong, C. Ren, M. Tian, X. Yang, J. Li and B. Li, Emulsion stability and dilatational viscoelasticity of ovalbumin/chitosan complexes at the oil-in-water interface, *Food Chem.*, 2018, **252**, 181–188.

43 A. F. H. Ward and L. Tordai, Time–Dependence of Boundary Tensions of Solutions I. The Role of Diffusion in Time–Effects, *J. Chem. Phys.*, 1946, **14**(7), 453–461.
44 S. Mad-Ali, S. Benjakul, T. Prodpran and S. Maqsood, Interfacial properties of gelatin from goat skin as influenced by drying methods, *LWT – Food Sci. Technol.*, 2016, **73**, 102–107.
45 C. Cheng, X. Yu, F. Geng, L. Wang, J. Yang, F. Huang and Q. Deng, Review on the Regulation of Plant Polyphenols on the Stability of Polyunsaturated-Fatty-Acid-Enriched Emulsions: Partitioning Kinetic and Interfacial Engineering, *J. Agric. Food Chem.*, 2022, **70**(12), 3569–3584.
46 H. Niu, W. Chen, W. Chen, Y. Yun, Q. Zhong, X. Fu, H. Chen and G. Liu, Preparation and Characterization of a Modified-beta-Cyclodextrin/beta-Carotene Inclusion Complex and Its Application in Pickering Emulsions, *J. Agric. Food Chem.*, 2019, **67**(46), 12875–12884.
47 H. Niu, W. Wang, Z. Dou, X. Chen, X. Chen, H. Chen and X. Fu, Multiscale combined techniques for evaluating emulsion stability: A critical review, *Adv. Colloid Interface Sci.*, 2023, **311**, 102813.
48 C. Le Bourvellec and C. M. Renard, Interactions between polyphenols and macromolecules: quantification methods and mechanisms, *Crit. Rev. Food Sci. Nutr.*, 2012, **52**(3), 213–248.
49 X. Pan, Y. Fang, L. Wang, Y. Shi, M. Xie, J. Xia, F. Pei, P. Li, W. Xiong, X. Shen and Q. Hu, Covalent Interaction between Rice Protein Hydrolysates and Chlorogenic Acid: Improving the Stability of Oil-in-Water Emulsions, *J. Agric. Food Chem.*, 2019, **67**(14), 4023–4030.
50 X. Yu, S. Chu, A. E. Hagerman and G. A. Lorigan, Probing the interaction of polyphenols with lipid bilayers by solid-state NMR spectroscopy, *J. Agric. Food Chem.*, 2011, **59**(12), 6783–6789.
51 J. Yu, M. Ahmedna, I. Goktepe and J. Dai, Peanut skin procyanidins: Composition and antioxidant activities as affected by processing, *J. Food Compos. Anal.*, 2006, **19**(4), 364–371.